Scripta METALLURGICA et MATERIALIA
Vol. 24, pp. 1759-1764, 1990
Printed in the U.S.A.

THE INFLUENCE OF MICROSTRUCTURE ON THE MACROSCOPIC PATTERNS OF SURFACE INSTABILITIES IN METALS

D. Rittel
Department of Mechanical Engineering
Yale University
New Haven, CT 06520-2157, USA
(Received July 6, 1990)

Introduction

The occurrence of surface instabilities on quasi-statically strained plastic solids is predicted by a theoretical analysis (see e.g. (1, 2)) and has been recently modelled by a finite element procedure (3). However, surface instabilities are seldom reported or identified as such in the experimental literature (4, 5). Whereas it is admitted that the microstructure of the deforming material has to play a role in the development of these instabilities, the subject remains largely unexplored. In this context, the "orange-peel" phenomenon, well known to metallurgists, has been identified as a type of surface instability corresponding to the development of surface waves in agreement with the bifurcation analysis for a material with low initial hardening coefficient (6). In a further analysis of the phenomenon, a systematic attempt has been made to characterize the wavelength of the surface features and its correlation to the average grain size of the material (7). The study comprised cast metals with a typical equiaxed microstructure (aluminum alloys and cast austenitic manganese steel).

The purpose of the present paper is to further establish our understanding of the microstructural contribution to surface instabilities.

Materials and Experimental

Two compression cylinders (approximate initial diameter to height ratio of 1:1) were machined, one from a bar of cast aluminum 1100, and the second from the same material, in the extruded condition. The cylinders were macroscopically smooth. Grooves were machined on the flat faces of the cylinders for minimal friction with the compressive plates (8).

Results and Discussion

Figure 1 shows the deformed cylinders. Both exhibit heavy surface roughening. For the cast material, this roughness is of "grainy" appearance and is evenly distributed over the cylinder. On the extruded material, a pattern of parallel wrinkles has developed but they are localized and restricted to the vicinity of the minor axes of the cylinder. These wrinkles are aligned with the compression axis which is also the cylinder's axis. It is also noted that the cast material retains its initial circular cross section upon compressive deformation whereas the cross section of the extruded material becomes elliptical.

0036-9748/90 $3.00 + .00

Figure 2 shows the characteristic microstructure of the starting materials. The extruded material is made of elongated (and almost indiscernible individual) grains which are aligned with the cylinder's axis on a longitudinal section. On a transverse section, the grains are elongated as well and the overall grain structure is similar to deck of playing cards. This observation shows the anisotropic character of the initial microstructure in the extruded sample. The microstructure of the cast material is characterized by equiaxed coarse grains with typical solidification dendrites visible at a slightly higher magnification. Here, the microstructure is isotropic, yielding similar features in longitudinal and transverse metallographic sections.

The tendency towards oval shape can now be understood in terms of initial anisotropy which causes anisotropic deformation. In addition, the localization of the wrinkles seems to indicate a higher level of surface straining in the vicinity of the minor axes of the specimen. For the initially isotropic cast material, the deformation response is isotropic as well, at least for the range of deformations imposed here.

It is also interesting to note the relationship between initial microstructure and the macroscopic pattern of surface roughness. Both types of patterns, i.e. grainy and wrinkled, are characteristic of surface instabilities; similar wrinkles have been observed to develop during internal pressurization of aluminum alloy cylinders (9). The present observations show that for a given material, wrinkles are not the only possible pattern of surface instabilities. Rather, wrinkles are characteristic of materials possessing an initial texture (such as extruded tubes or rolled sheets) the way "orange-peel" is characteristic of equiaxed microstructures. This point is further supported in another material (aluminum-lithium alloys (10)): the figures shown in this paper show that little initial texture yields a grainy type of instability whereas materials possessing a higher degree of texture exhibit a wrinkled pattern upon deformation.

So far, it has been shown that there are several possible macroscopic patterns of surface instabilities which are dictated by the initial microstructure of the material. Furthermore, as shown in the present and previous work, it would be desirable to incorporate a length scale into the description of surface instabilities. Current continuum analyses do not contain (nor do they predict) length scales; these are imposed *a-priori* in existing models as geometrical initial imperfections whose evolution with deformation is studied.

An alternative approach, similar to the approach of (3), is to assume a solution for the velocity field associated with the surface instability. Here, microstructure-related evidence is to be incorporated wherever possible. The general description of the field is chosen to be three-dimensional with exponential decay of the amplitude with increasing depth, as the characteristic of surface waves:

$$V_1 = A\, e^{-\alpha x_3} \exp[\, ik(x_1 - x_{10})]$$
$$V_2 = B\, e^{-\alpha x_3} \exp[\, ik(x_2 - x_{20})] \qquad <1>$$
$$V_3 = V_1 + V_2$$

Where V_1 and V_2 indicate waves propagating in the 1 and 2 direction with respective phases X_{10} and X_{20}. K, the wavenumber, is equal to $2\pi / \lambda$, where λ stands for the wavelength. The natural length scale can be introduced via the wavelength of the instability, as follows:

The rate of decay is set by a constant, α, which is assumed to be inversely proportional to λ, say $\alpha = ct. / \lambda$. Previous observations (6, 7) have shown that surface roughness scales with the average grain size. The latter sets the wavelength for a given material, and it is therefore reasonable to assume that the amplitudes A and B are functions of λ. Accordingly, $A = n\lambda$ and $B = m\lambda$. Equation <1> becomes:

$$V_1 = n\lambda\, e^{-\frac{ct.\, x_3}{\lambda}} \exp\left[i\frac{2\Pi}{\lambda}(x_1 - x_{10}) \right]$$
$$V_2 = m\lambda\, e^{-\frac{ct.\, x_3}{\lambda}} \exp\left[i\frac{2\Pi}{\lambda}(x_2 - x_{20}) \right] \qquad <2>$$
$$V_3 = V_1 + V_2$$

The relationship between microstructure and surface instability is further embodied by the ratio n/m (or its inverse). The aspect ratio R (height over width of a grain in a given metallographic section) is equal to unity for an equiaxed structure corresponding to isotropic behavior. In the case of elongated grains, the aspect ratio increases accordingly. Since the present observations show a correlation between the aspect ratio of the grains and the macroscopic aspect of the associated surface instability, it is proposed that R = n/m.

Figure 3 shows a plot of the surface described by equation <2> at $X_3 = 0$ for R = 1 and R = 20 (arbitrary value), λ being constant. The patterns rendered in this figure simulate reasonably well the actual macroscopic textures observed on the samples.

As a final remark, it should be noted that while some information is available for equiaxed microstructures, additional research is needed to determine the wavelength of the wrinkles as a function of the microstructure.

Conclusions

The macroscopic aspect of surface instabilities is closely related to the initial microstructure (and degree of isotropy) of the deformed material. Accordingly, an attempt has been made to incorporate microstructural parameters (wavelength, aspect ratio of the grains) into the equations describing the instability. The character of the equations remains unchanged while including salient features of the observed instabilities at both continuum and microstructural levels.

Acknowledgments

The experimental specimens were generously provided by Dr. P.R. Dawson. The author would like to thank Dr. E.W. Bolton for discussing the manuscript.

References

1. R. Hill and J.W. Hutchinson, *J. Mech. Phys. Solids*, **23** (1975) 239.
2. J.W. Hutchinson and V. Tvergaard, *Int. J. Mech. Sc.*, **22** (1980) 339.
3. J.P. Bardet, *Comp. Meth. in Appl. Mech. and Engrg.*, **78** (1990) 270.
4. O.A. Onyewuenyi and J.P. Hirth, *Metall. Trans. A.*, **13** (1982) 2209.
5. A. Valkonen, A. Chatterjee and J.P. Hirth, *Int. J, Mech. Sc.*, **29** (3) (1987) 219.
6. D. Rittel and I. Roman, *Matls. Sc. and Engrg.*, **A110** (1989) 77.
7. D. Rittel, R. Aharonov, G. Feigin and I. Roman, *submitted for publication* (1990).
8. P.R. Dawson, *Private Communication* (1990).
9. M. Larsson, A. Needleman, V. Tvergaard and B. Storakers, *J. Mech. Phys. Solids*, **30** (3) (1982) 121.
10. P.J. Gregson, D.S. McDermaid and E. Hunt, *Matls. Sc. and Tech.*, **4** (1988) 713.

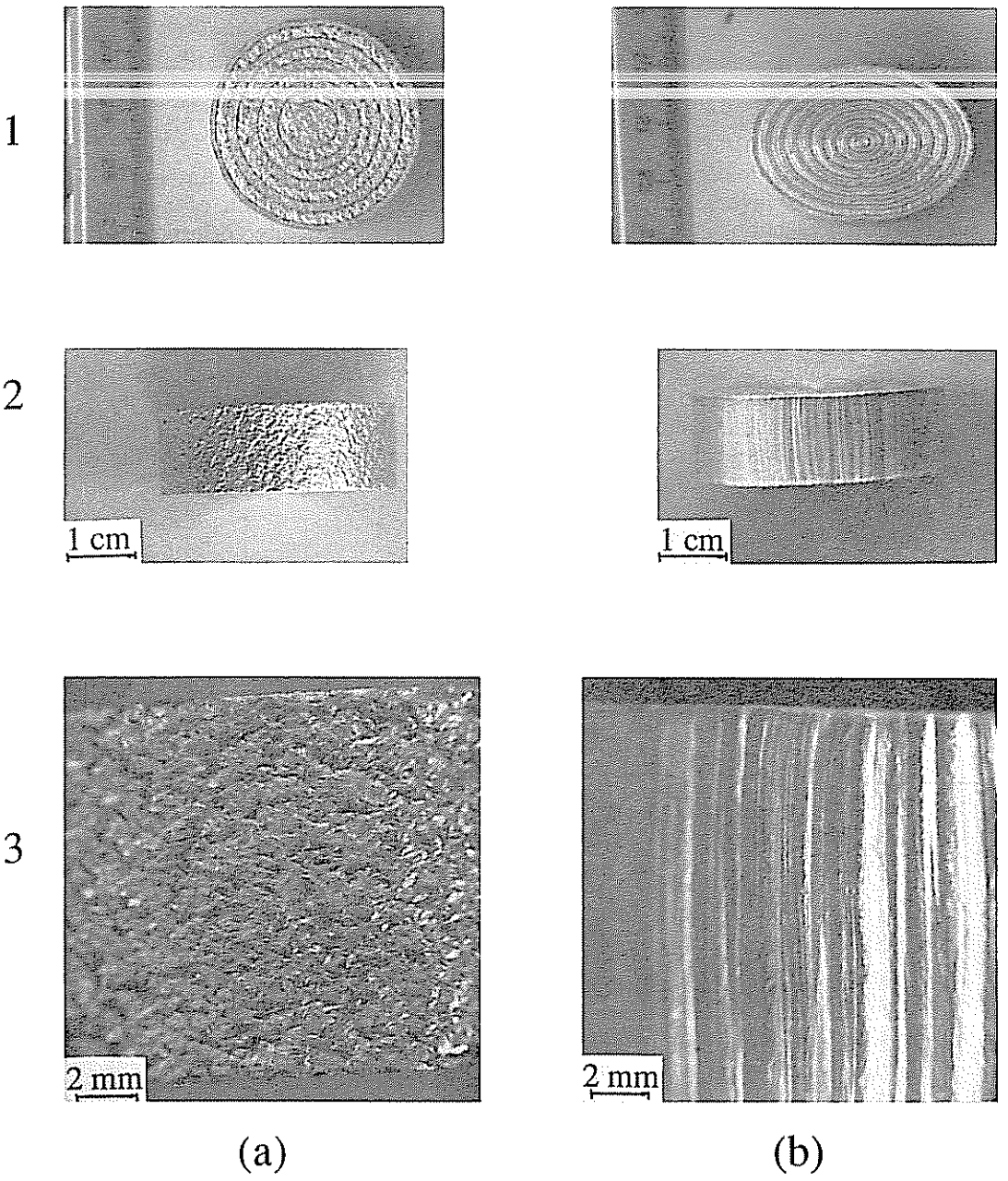

Figure 1: Compressed 1100 aluminum cylinders. Grooves are made for lubrication.
(a) Cast material. 1: Top view, 2: Side view, 3: Magnification of the surface pattern.
(b). Extruded material. 1, 2 and 3: as above.

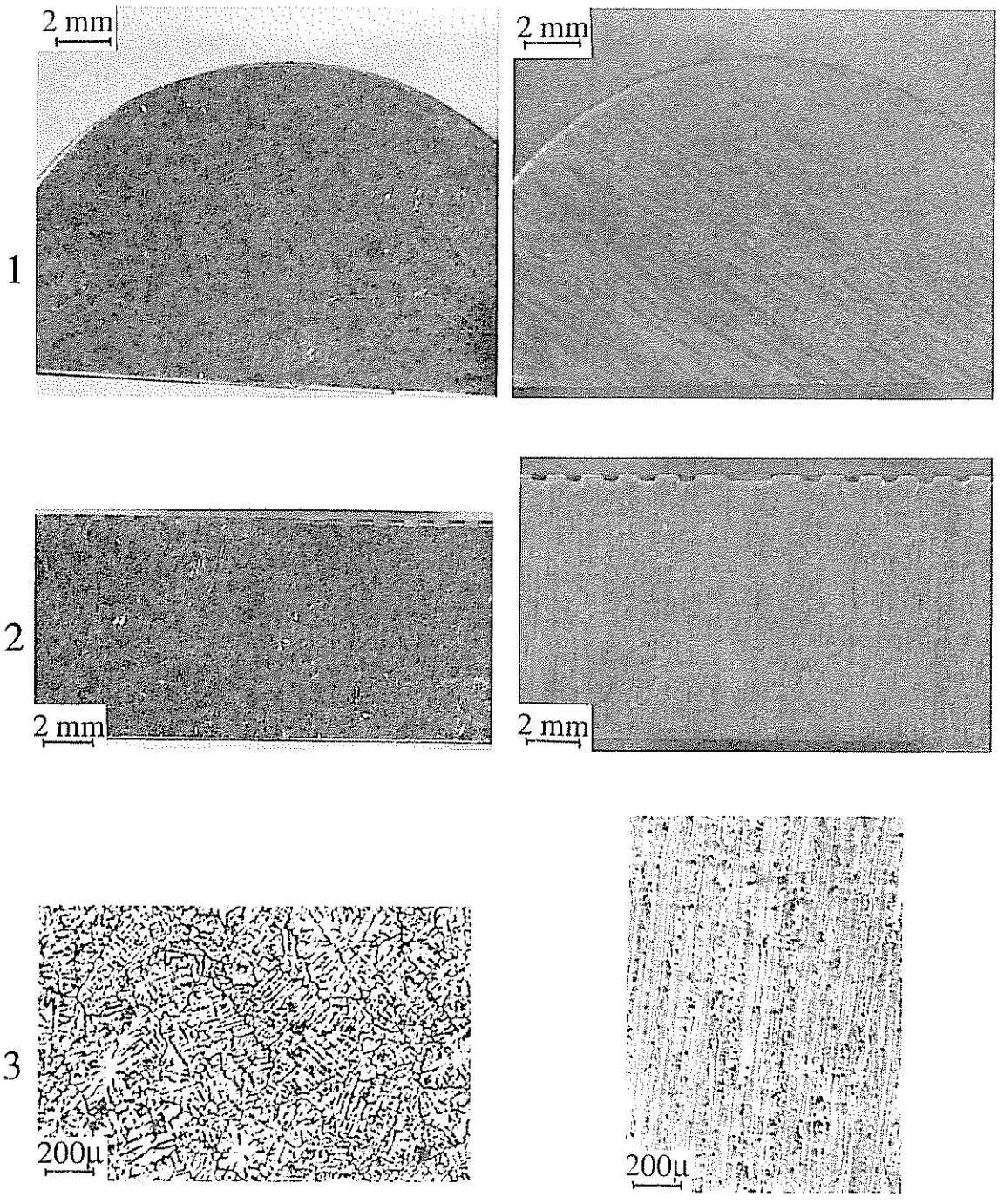

Figure 2: Typical microstructures. Etchant: mixed acids.
(a) Cast material. 1: Transverse section, 2: longitudinal section, 3: Magnification.
(b) Extruded material. 1, 2 and 3: as above.

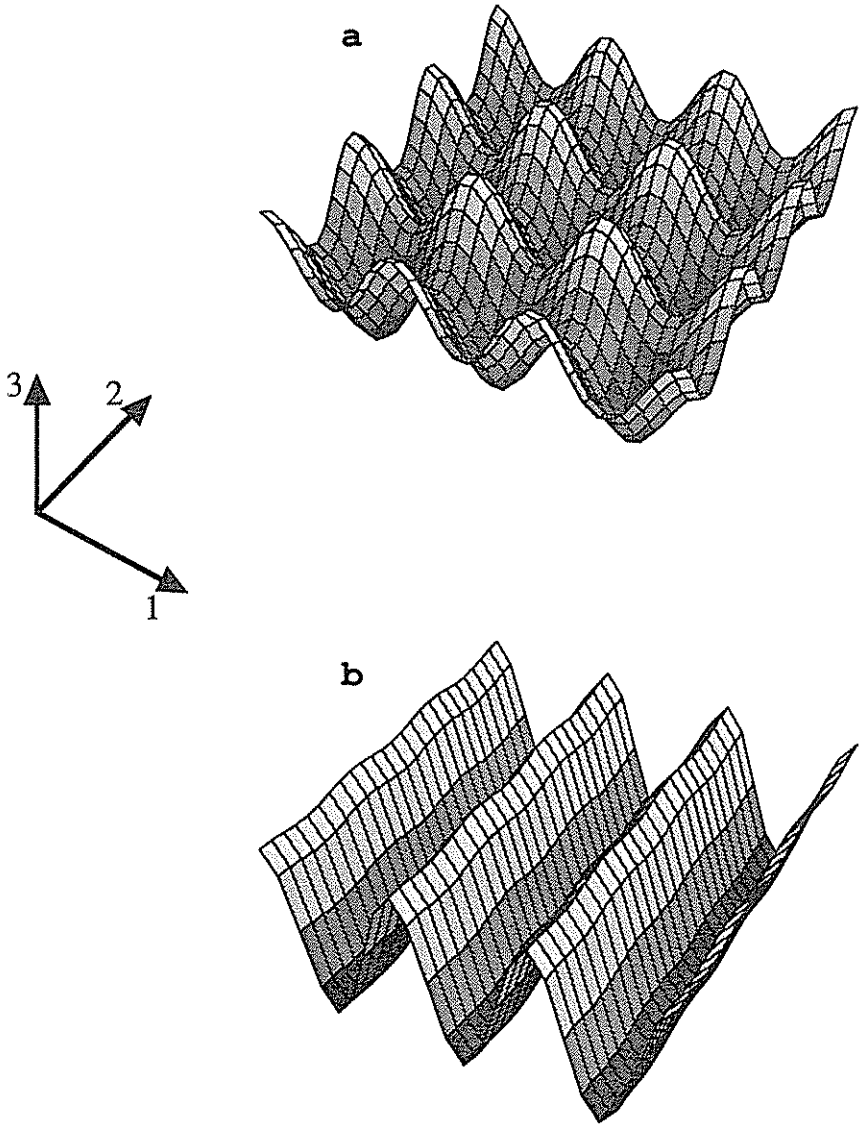

Figure 3: Simulated patterns of surface instabilities using equations <2>, at X3 = 0, and compression along X2 axis.(a) R = 1, (b) R = 20.